GEOMETRIC CORRECTION MODEL FOR THE GENERATION OF TERRAIN CORRECTED PRODUCTS

N. Padmanabhan and K. L. Majumder
Image Processing and Products Division
Image Processing and Data Products Group
Space Applications Centre
Jodhpur Tekra
Ahmedabad 380053
INDIA

ABSTRACT

A method for generating a fully corrected product, incorporating the terrain variations, of remotely sensed images is presented. The terrain variations are modelled by a two dimensional surface locally. Decreasing the local window representing the terrain variations, improves the accuracy of the method. The method is very useful for generating fully corrected products of remotely sensed data, particularly when the satellite is sidelooking. The method can also be used for generating orthoimages.

Key words: Geometric correction, modelling, terrain correction.

INTRODUCTION

Geometric correction is an essential step for the proper interpretation and utilisation of remotely sensed images. However, most of the corrections incorporated so far have been to compensate for the orbit and attitude variations of the satellite. This type of correction is sufficient so long as the satellite is nadir looking. But the SPOT series of satellites and the IRS 1C/1D satellites have sidelooking capability. The sidelook geometry introduces panoramic distortions, proportional to the look angle and the terrain variations, which need to be corrected for. Besides, attempts have also been made in recent times to merge data from different optical sensors like NOAA and SPOT (Moreno et al (1992)). Also, with the proliferation of geostationary satellites, some interesting possibilities arise, regarding merging of fine spatial but coarse temporal resolution data, with fine temporal but coarse spatial resolution data. For all this type of data merging, first it is necessary to correct the data for its specific imaging geometries. For instance, if the two sensors which are being combined, have different look angles, the panoramic distortions arising in the two different images have to be removed before merging is attempted. This is all the more important when the images being combined correspond to hilly terrains. In plain terrains, the panoramic distortions are not significant, though not negligible. However, when the terrain is hilly, the panoramic distortion is quite significant. In fact, a plateau of 2 km above the reference surface, will give a shift of about 300 metres in the across track direction for look angle of 26° (Marvin et al (1987)). Thus, when it is desired to generate a geometrically corrected product of accuracies of about 10 metres or less, corrections for these types of distortions are essential. Further, with the launch of the ERS satellite, data is available in the microwave band as well. Hence, it is natural to try to combine this data with the data from the optical sensor (Yao and Gilbert (1984)). The microwave imagery is always sidelooking, with a fixed sidelooking angle, whereas, the optical sensor can be nadir or sidelooking. Thus, in this case also correction of terrain related distortions is called for.

One of the simplest ways of doing this correction is to identify some reasonable number of Ground Control Points GCPs in the image, and use a warping polynomial (Kientz et al (1993)). In fact, this method was used recently by Welch et al (1985), to generate an anaglyph product. The method works reasonably well in plain terrains, but is found inadequate in hilly terrains, due to the following reasons:

a) Difficulties in identification of GCPs particularly in hilly terrains;

b) A warping polynomial, whatever be the degree, will not represent the distortions adequately in the entire image.

To overcome the second problem, recently Goshtaby (1988) has proposed a method. In his approach, he has assumed a slightly more complicated functional representation, instead of a simple polynomial.

But in all the methods involving GCPs, the problem of selecting the control points remain. To overcome these problems, Marvin et al (1987) have suggested an iterative method on the conventional Look Point Equation. They have linearised the representation of earth surface locally to achieve fast convergence.

More recently, Itten and Meyer (1993), have given a method for removing the terrain related distortions to improve the accuracy in classification. The authors have given a very simplistic approach for finding out the actual point imaged, knowing the terrain variations in the area of interest. They have approximated the earth by a sphere, and assumed that the shift

in the point imaged, due to terrain variations will be along a circular arc. However, this is not strictly correct. The earth being a spheroid, the section by a plane is not always a circle. Besides, the shift will be in a plane containing the detector array and the principal point, and hence will depend on the attitude of the satellite.

In this paper, we propose a new method for incorporating the terrain variations in generating a fully corrected product. The problem formulation and the methodology for obtaining the point imaged incorporating the terrain variations are given in Section II. The optimisation procedure for doing the same and the methodology for generating a fully corrected product incorporating the height variations are given in the same section. In Section III some test results are presented, while in Section IV the merits and limitations of the method vis a vis the other existing methods are discussed. Section V presents an error analysis of the method, while Section VI contains some concluding remarks, and the modification needed for using the technique given in the paper for other type of sensors like LANDSAT.

II FORMULATION

It is assumed that the input image is the radiometrically corrected data - image data corrected for line and pixel dropouts, and sensor normalized. The problem is to generate a fully corrected product, say a Geocoded Product, incorporating corrections for terrain related distortions.

The area of interest A is specified in terms of the corner latitudes and longitudes (ϕ_i, λ_i), i = 1,2,3,4, while the input space I is defined in terms of the pixel and scanlines

$$(p_i,s_i),\ i = 1,2,3,4.$$

Thus,

$$I: \quad p_1 < p < p_2 \ , \quad s_1 < s < s_2 \ ,$$

$$p_1 = p_3 \ , \ p_2 = p_4, \quad s_1 = s_2 \ , \ s_3 = s_4 \qquad \ldots\ldots (1)$$

and

$$A: \quad \phi_3 < \phi < \phi_1 \ , \quad \lambda_1 < \lambda < \lambda_2 \ ,$$

$$\phi_1 = \phi_2 \ , \ \phi_3 = \phi_4 \quad \lambda_1 = \lambda_3 \ , \ \lambda_2 = \lambda_4 \qquad \ldots\ldots (2)$$

The terrain variations is assumed to be known in terms of a Digital Elevation Model (DEM) of the area of interest at the desired sampling interval. Guindon (1993) has presented the sampling requirements of DEM so that the final product is within a given specification. It is shown that for SPOT, to achieve an error tolerance of 12.5 metres, DEM sample spacing should be about 15". The problem is to assign gray values to each of the output pixel in the area of interest A, from the corresponding locations in the input space I, after incorporating the terrain variations.

The first step in the generation of the said product is to establish a relationship between the output space and the input space. Using map projection, the area of interest A, which is in the ground coordinates space is converted to the output space O, and is defined as $(xout_i, yout_i)$, i = 1,2,3,4, where $xout_i$, $yout_i$, are the map projection coordinates.

Thus,

$$O: \ \min(xout_i) < xout < \max(xout_i)$$

$$\min(yout_i) < yout < \max(yout_i)$$

$$i = 1,2,3,4 \quad \ldots\ldots (3).$$

Thus, given any (x, y) in the output space, it is desired to find the corresponding locations (p, s) in the input space, so that proper gray values can be assigned to the output location.

Various approaches have been tried in the past for establishing such a relationship, the simplest one being the use of warping polynomials. As mentioned earlier, this does not give sufficiently accurate results, and hence there is a need to look at the problem afresh.

The input and the output spaces are related by a one to one mapping

$$O \rightarrow I: \quad p = f(x,y)$$

$$s = g(x,y), \quad (x,y) \varepsilon\ O \ \ldots (4)$$

However, this relationship has got nine parameters, namely the position vector of the satellite, velocity vector of the satellite and the attitude values, roll, pitch and yaw, which are all functions of time. Besides, the shape of the earth cannot be described by a simple mathematical function, particularly when the terrain variations are to be introduced. Establishing such an output to input relationship without using a warping polynomial is not simple. Hence, using the geometry of the imaging conditions, we first establish a relationship between the input space and the ground as

$$I \rightarrow G: \quad \phi = f(p,s)$$

$$\lambda = g(p,s) \ , \ (p,s,) \varepsilon\ I \ldots (5)$$

A. Image to Ground Mapping

In the present work, we start with the assumption that the imaging can be modeled by a Pin Hole type of geometry. This means, that the point on the ground imaged by a particular detector is the point of intersection of the earth and the straight line joining the detector in question and the principal point . This assumption leads us to the derivation of the Look Point Equation (LPE). We first start with the LPE for the smooth earth surface.

We define the following systems of coordinates:

1: Inertial System of Coordinates:

x axis is along the First Point of Aries Γ true of date

z axis is the axis of the earth's rotation

y axis is chosen that they form a right handed system of coordinates; Origin is the centre of the earth.

This system should be the one in which the satellite state vectors are obtained.

2: Orbital system of coordinates:

z axis is $-\mathbf{R}$

y axis is $-\mathbf{R} \times \mathbf{V}$

x axis is $(\mathbf{R} \times \mathbf{V}) \times \mathbf{R}$

Here $\mathbf{R}$ and $\mathbf{V}$ are the position and velocity vector of the satellite.

3: Spacecraft system of coordinates:

Origin is the point of intersection of the principal axis and the detector array;

y axis is the detector array

z axis is the principal axis

x axis chosen so that they form a right handed system;

4: Payload system of coordinates:

This system is same as above, but the axes are rotated through the look angle about the corresponding axis.

In the inertial system of coordinates, the smooth earth is represented by the following equation:

$$x^2/a^2 + y^2/b^2 + z^2/c^2 = 1 \quad \ldots\ldots (6)$$

where a,b,c are the parameters of the spheroid representing the earth.

In view of the above choice of the coordinate systems, any point whose coordinates in the Payload system of coordinates are (x^{pl},y^{pl},z^{pl}), can be converted to the inertial system of coordinates as follows:

$$(x^{in},y^{in},z^{in}) = MPL * MS * MO * (x^{pl},y^{pl},z^{pl})^t + (x^{sp},y^{sp},z^{sp})^t \quad \ldots\ldots (7)$$

where $(x^{sp},y^{sp},z^{sp})^t$ is the position vector of the satellite in the inertial frame of reference. MPL, MS,MO are the transformation matrices representing the transformations from the payload system to spacecraft system to orbital system respectively.

Let us consider detector number p. Using the parameters of the sensor, the coordinates of this detector in the payload system of coordinates are found out, and let them be $(x^{pl}_p,y^{pl}_p,z^{pl}_p)$. Using equation (7), the coordinates of the said detector in the inertial system of coordinates are obtained as $(x^{in}_p, y^{in}_p, z^{in}_p)$. The same calculations are done for the principal point, thus obtaining the coordinates of the same in the inertial frame as $(x^{in}_f,y^{in}_f,z^{in}_f)$. Under the Pin Hole camera assumption, the detector under consideration will image the ground point obtained by the intersection of the line joining these two points with the earth surface.

The equation to the line joining these two points is

$$(x - x^{in}_p)/(x^{in}_f - x^{in}_p) = (y - y^{in}_p)/(y^{in}_f - y^{in}_p) = (z - z^{in}_p)/(z^{in}_f - z^{in}_p) \quad \ldots\ldots (8)$$

This, when solved with equation (6) , gives the coordinates of the point P' (Figure 1) on the ground imaged by the detector. The inertial coordinates of P' are converted to the ground coordinates of ϕ and λ using the transformations involving sidereal angle. This establishes a direct mapping from the input space I to the ground space G. Using map projection transformations, this can be transformed in to input space to output space mapping.

B. Incorporating the height in the image to Ground Mapping

As explained above, the ground coordinates of the point imaged by any pixel can be found out. However, since the earth itself is modeled as a smooth spheroid, the point imaged will not include the terrain variations. To be more realistic with the terrain effect, the shape of the earth should be modeled by a surface, which is a true representation of the earth surface.

However, representing all the terrain variations by a surface is very difficult , if not impossible. Hence, we will approximate the same by a bilinear surface locally. For this, it is assumed

that the point imaged using the smooth ellipsoid model is P' (ϕ,λ). Converting these geodetic coordinates into map projection coordinates and using this point as centre a window W of size (n x n) is chosen. Let the corners of this window be A,B,C and D. Reading the heights from DEM at these points, the true points A',B',C' and D' of the window including the terrain variations are obtained in the inertial frame (Figure 1). With these four points a bilinear surface is fitted as follows :

$$E: z = ax + by + cxy + d \quad \ldots\ldots (9)$$

This bilinear surface is thus an approximate representation for the earth near P'. Obviously, more the variability of the terrain, greater will be the deviation of the bilinear fitted surface from the actual surface. However, depending upon some preassigned threshold value, the size of the window can be reduced, or increased, so that the deviation of the bilinear surface from the true earth surface is within the threshold value.

This surface is now used in solving the Look Point Equation. Suppose P" is the point of intersection of the Look Point Vector with the bilinear surface. From P", let P"N be a normal to the earth ellipsoid. Then, P'N, gives the shift in the ground position imaged. However, solving over an entire window will give very coarse results. Hence, the window W is divided into smaller surfaces w_i with corners A_i,B_i,C_i and D_i. For each of these sub windows, the Look Point Equation is solved. Suppose for the subwindow w_i, the point of intersection with the straight line (8) is (x_{wi}, y_{wi}, z_{wi}). It is made sure that this point lies inside the subwindow and not outside. Of all the subwindows which have such an intersection, the one which is closest to the satellite contains the actual point of intersection of the straight line and the window W. Let this point be $\pi'(x,y,z)$. From this point a normal is drawn to the surface of the smooth earth. The ground coordinates of the foot of this normal N, will be the ground coordinates of π'. The distance between π' and N, gives the height component.

Though the above mentioned method gives good results, it is very time consuming. In fact, an experiment was performed and the time taken was estimated to be around 20 seconds per point. This is too high a figure and hence we have attempted to optimise the same .

The four corners of the window W are used to fit a bilinear surface as mentioned above. Outside this, the surface is extended by a plane surface,

$$E: z = \min(z_a, z_b, z_c, z_d) \quad \ldots\ldots (10)$$

Thus, the earth is modeled locally as

$$S = S\,U\,E \quad \ldots\ldots (11)$$

The straight line defined in equation (8) is solved with the equation (11). Let the point of intersection be (x,y,z). From this point a normal is drawn to the earth spheroid. Let the foot of the normal be N. A check is made to see if the point N is within the window. Around this point N, a window of size (n/2 x n/2) is chosen, and the same process is repeated till the window size becomes (1 x 1). At this stage, the foot of the normal N gives the point on the earth surface, whose ground coordinates should be assigned to the pixel P. The distance N gives the shift due to the terrain variations.

C. Output to input mapping

However, in order to generate a Geocoded product, what is needed is a reverse mapping from the output space O to the input space I. Given a point (ϕ,λ) in the output space, to find the corresponding point (p,s) in the input space I, which would have imaged this point. In view of the dependence of nine parameters, it becomes an iterative problem on nine parameters. One way of avoiding this is to establish an a priori functional form for satellite positions, velocity and the attitude in terms of time, and then use this functional form to determine the values of these variables at any time. Thus, the iteration can be reduced to only two variables, namely time and pixel number. However, this would call for the calculation of the satellite state vector and attitude values from the functional form established a number of times, leading to an enormous computational effort. Besides, when we want to introduce the terrain related variations, the problem is almost unmanageable in this way, for the terrain variations introduce two more dimensions. Hence, we propose to use the simple direct mapping established above for the desired inverse mapping. For this, the input space is divided into primary grids of size m x m. For each of these primary grid points, the procedures mentioned above are applied and the ground coordinate of the point imaged is obtained. The output space O, which is defined in equation (3) is divided into primary grids of sizes (n x n). For each of these primary output grids, the map projection coordinates are calculated. In order to find out the input location corresponding to these primary grids, their map projection coordinates, the xout, yout are compared with the same in the input space. This search gives the primary grid in the input space I in which this output grid lies. Knowing the input pixel and scanline number of the four corners of the input primary grid in which this output grid falls, and using a bilinear interpolation, the pixel position in the input space corresponding to a given point in the output space is obtained. This procedure is adopted for all the primary grids in the output space, and thus their corresponding input locations are found out.

III TEST RESULTS

The above mentioned methodology was tested for an area where the heights range from 150 to

350 metres. Two sets of data were used - IRS 1C Panchromatic data. We consider various detector elements, the shift due to the terrain variations was observed. The shifts observed were of the order 4 metres in nadir case and of the order of 120 metres along parallels and about 19 metres along meridians were observed. The shifts along parallels and along meridians for points imaged in three different scanlines are shown in Figures 2 and 3. The heights at the same points are given in Figure 4. It can be observed that the shifts obtained are not simple bias, but are functions of height. In Table 1, we have given the shifts and heights corresponding to various pixels of two different lines. It can be seen that for the same shift, for two different pixels P1 and P2, P1 > P2, the height corresponding to P2 should be less.

This is easily explained in Figure 5. Figures 6 and 7 give the shifts in the along parallel and along meridianal directions for the various pixels in the input space. The points depicted correspond to various points in the input space, which can be identified by their Easting and Northing coordinates. The points are at intervals of 64 pixels and 64 scanlines.

Table :1 Shifts and heights at various pixel posifions at different scan lines

Scan number	Pixel number	Shift along parallel (met)	Shift along meridian (met)	Height (met)
193	1	129.99	-20.46	288.23
193	129	136.18	-21.44	304.69
193	257	130.05	-20.47	289.72
193	385	131.35	-20.69	296.71
193	513	124.48	-19.60	279.85
193	641	130.50	-20.56	296.31
193	769	122.44	-19.29	278.35
193	897	159.17	-25.11	373.83
193	1025	122.58	-19.32	281.64
193	1153	121.66	-19.18	281.64
193	1281	114.97	-18.18	265.48
193	1409	114.64	-18.08	266.08
769	1	122.70	-19.32	271.17
769	129	121.41	-19.59	270.57
769	257	120.31	-18.95	268.47
769	385	122.52	-19.30	273.86
769	513	127.44	-20.09	291.52
769	641	116.07	-18.29	268.08
769	769	118.58	-18.68	270.27
769	897	116.59	-18.38	266.98
769	1025	120.23	-18.96	276.85
769	1153	121.95	-19.24	284.04
769	1281	118.31	-18.67	277.75
769	1409	112.32	-17.72	261.29

displacements at the various input locations being very small (of the order of 100 metres along parallels and of the order of 10 metres along meridians), we have instead plotted (shift_along_parallel - 110)*75 in Figure 6 and (shift_along_meridian + 16)* 250 in Figure 7. These figures also reflect the functional dependence of the shifts on the heights as mentioned above. With these Image Ground Mapping results corrected for the terrain variations, we have used the output to input mapping to obtain the pixel positions corresponding to each of the primary grid of the output space. For comparison, the same is done for the smooth ellipsoid model also. Using these two mappings, we have generated two Geocoded products, one incorporating the terrain variations, and the other without incorporating the same. The shift of about 120 metres in the input locations due to terrain correspond to about 4 pixels in the output space.

IV DISCUSSIONS

We have presented a method for the generation of a fully corrected product incorporating the terrain variations. Thus the method can be used to generate orthoimage. Besides, if a product with terrain corrections from two different Look angles are combined, an anaglyph product can be generated. The method is quite fast and has been implemented in a Silicon Graphics Workstation.

The method presented here has got the advantage of better accuracy and gives the shift in the point imaged due to terrain in the correct plane of imaging. In fact, the present method gives the shift in the across track and along track directions, the former being naturally larger. Also the shift formulation is not dependent on a circular arc approximation as in Itten et al (1993). Besides, even in the nadir looking case, the method is able to give the shift, even though it is insignificant.

The method given for height incorporation could have been initiated with one bilinear surface of size 25 m x 25 m surrounding the point P'. However, in such a case, the point of intersection might lie in the surface extended rather than the surface itself. To avoid this, we have chosen an initial window of size 128 x 128 grids, each of 25m resolution. To speed up the process, we have represented the earth surface by a bilinear surface inside a window, but extended it by a plane outside. This is because, depending upon the variations in height, sometimes the straight line from the detector through the principal point, in LPE, might not intersect the bilinear surface at all. This is particularly true if the window has a valley region within. By extending the surface, a finite point of intersection is always ensured. Since at any stage, the window size is half that at the previous stage, the correct point will be obtained in 9 steps (except when the intersection is with the extended plane, rather than the bilinear surface, in which case the window will be shifted without reduction in size), as compared to 128 x 128 steps in the direct method. Thus, we have been able to accelerate the convergence of the method exponentially.

Even though we have so far considered Geocoded products only, the method presented here is general enough to generate bulk corrected products as well. In such a case, the output space has to be fixed as follows:

Corresponding to the four corners of the input image, the ground coordinates (ϕ_i, λ_i), i=1,2,3,4, are found out. These are converted into map projection coordinates (x_i,y_i). Since, in bulk corrected products, the satellite track is taken as one of the axis, we define a new system of coordinates (x',y'); x' makes an angle θ with x axis, as shown in Figure 8. The angle θ is obtained from the formula

$$\theta = 0.5 \left[\tan^{-1}((y_2-y_1)/(x_2-x_1)) + \tan^{-1}((y_3-y_4)/(x_3-x_4)) \right] \quad \ldots\ldots (12)$$

Thus the y' axis is now along the satellite track. The outputspace corners (x_i,y_i) are now converted to x',y' system by the formula

$$\begin{aligned} x'_i &= x_i \cos\theta - y_i \sin\theta \\ y'_i &= x_i \sin\theta + y_i \cos\theta \end{aligned} \quad \ldots\ldots (13)$$

Let

$$x'_{min} = \text{minimum } (x'_i)$$

$$x'_{max} = \text{maximum } (x'_i)$$

$$y'_{min} = \text{minimum } (y'_i)$$

$$y'_{max} = \text{maximum } (y'_i) \quad i = 1,2,3,4 \quad \ldots\ldots (14)$$

Then the output space is defined as

$$\begin{aligned} x'_{min} < x' < x'_{max} \\ y'_{min} < y' < y'_{max} \end{aligned} \quad \ldots\ldots (15)$$

For establishing the output to input space mapping, first the x',y' coordinates are converted to x, y coordinates using the inverse of equation (13) , and then the search in the input space is started.

V ERROR ANALYSIS

The sources of errors in the method described in this paper are:

1. Image to Ground Mapping:

In this step, the errors arise due to the inaccuracy of the orbit and attitude information. However, this error can be removed by using some Ground control points. The error introduced at this stage is the same as in orbit and attitude determination and hence can be quantified.

2. Height Incorporation:

In this step, the error introduced will be due to the fitting of a bilinear surface to represent the earth locally. Thus, if the variation in height is high, then it will be necessary to decrease the resolution element.

3. Output to Input mapping:

In this step, the error introduced will be due to the fitting of a bilinear surface connecting the input space and the output space. The error is proportional to the window size. In our study, we have chosen a window size of 64 x 64, so that the error is of the order of 0.01 pixel.

4. Resampling introduces error of the order of 0.01 pixel.

VI CONCLUSIONS

A new method of modelling for geometric correction, incorporating the terrain variations has been presented. The method presented is general enough and can be used to generate geometrically corrected products of areas, which lie in more than one scene. In fact, even if part of the area is imaged by one sensor and the other part by another sensor, then also the method can be used to generate a geometrically corrected product of the area of interest. Work in generation of the fully corrected products using IRS 1D data is underway.

We have considered only LISS type of sensor. However, the method is applicable to LANDSAT type of sensors also. In such a case, the Image to Ground Mapping model should incorporate the scanning mechanism also. It is to be noted that the entire methodology is very much suited for sidelook geometry. However, in such a geometry, the refraction effect due to the atmosphere plays a crucial role. It can be shown that the effect of refraction is a displacement of about 160 metres when the sidelook angle is about 26°. This effect also has to be incorporated if the accuracy of the product is to be enhanced. Work in this direction has been initiated, and will be reported in a subsequent paper.

ACKNOWLEDGEMENTS

The authors are grateful to the Group Director, Image Processing and Data Products Group for his constant encouragement. We are also thankful to the Director, Space Applications Centre, for providing us with the necessary facilities to complete the work reported. Thanks are also due to the staff of the Computer Centre for providing us with the computing facilities.

REFERENCES

1. Goshtaby, A, " Registration of images with geometric distortions", IEEE Trans. Geosci. and Remote Sensing, vol 26, 60 - 64, 1988

2. Guindon, B, "Derivation of digital evaluation data requirements for operation

satellite image coding", Proc. Int. Symp. Operationalisation of Remote Sensing, 19 - 23 April 1993, vol 6, ed., JL van Gendersen, RA van Zeidan and C Pohl, 1 - 13.

3. Itten, KI and Meyer, P, "Geometric and radiometric corrections of TM data of mountainous forested areas", IEEE Trans. Geosci. and Remote Sensing, vol 31, 764 - 770, 1993.

4. Kientz, B, "Advanced Image Processing workshop: interest of an advanced geometric correction system to produce Remote Sensing Geocoded Data", Proc. Int. Symp. Operationalisation of Remote Sensing 19 -23 April 1993, vol 6, ed., JL van Gendersen, RA van Zeidam and C Pohl, 177 - 188.

5. Marvin, JW, Labovitz, ML and Wolfe RE, "Derivation of a fast algorithm to account for distortions due to terrain in earth viewing satellite sensor images", IEEE Trans. Geosci. and Remote Sensing, vol 25, 244 - 251, 1987.

6. Moreno JF, Gandia S and Melia J, "Geometric integration of NOAA AVHRR and SPOT data: Low resolution effective parameters from high resolution data", IEEE Trans. Geosci. Remote Sensing, vol 80, 1006 - 1014, 1992.

7. Welch R, Jordan T and Lewall JC, "Geocoding and stereo display of tropical forest multisensor data sets", PERS vol 56, 1389 - 1392, 1990.

8. Yao SS and Gilbert JR, "Registration of a synthetic aperture radar image to TM imagery for Remote Sensing Applications", IEEE Trans. Geosci. and Remote Sensing, vol 22, 559 -563, 1984.

List of Figures and their captions:

Figure 1. Schematic diagram of terrain related correction procedure

Figure 2. Shift along parallels for various pixels of three different lines

Figure 3. Shift along meridians for various pixels of three different lines

Figure 4. Height variation for various pixels of the same three lines as in Figures 2 and 3.

Figure 5. Schematic diagram showing the dependence of shift on height and the pixel position.

Figure 6. Shift along parallels in the entire input image at grids of 64 pixels by 64 scanlines intervals;

shift = 75 * (shift_along_parallel - 110)

Figure 7. Shift along meridians in the entire input image at grids of 64 pixels by 64 scanlines intervals;

shift = 250*(shift_along_meridian + 16)

Figure 8. Fixation of output space for bulk corrected product generation

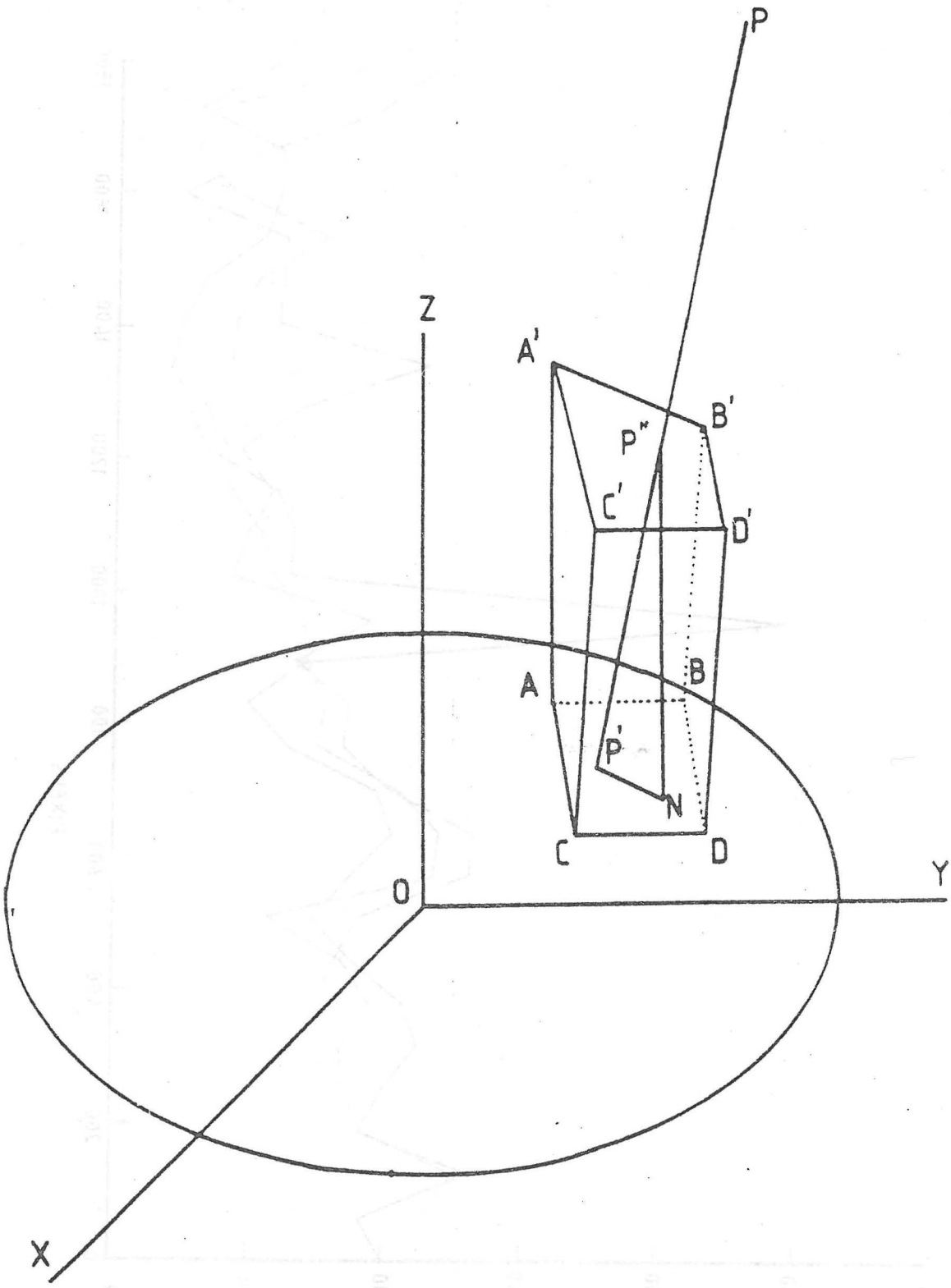

FIG. 1

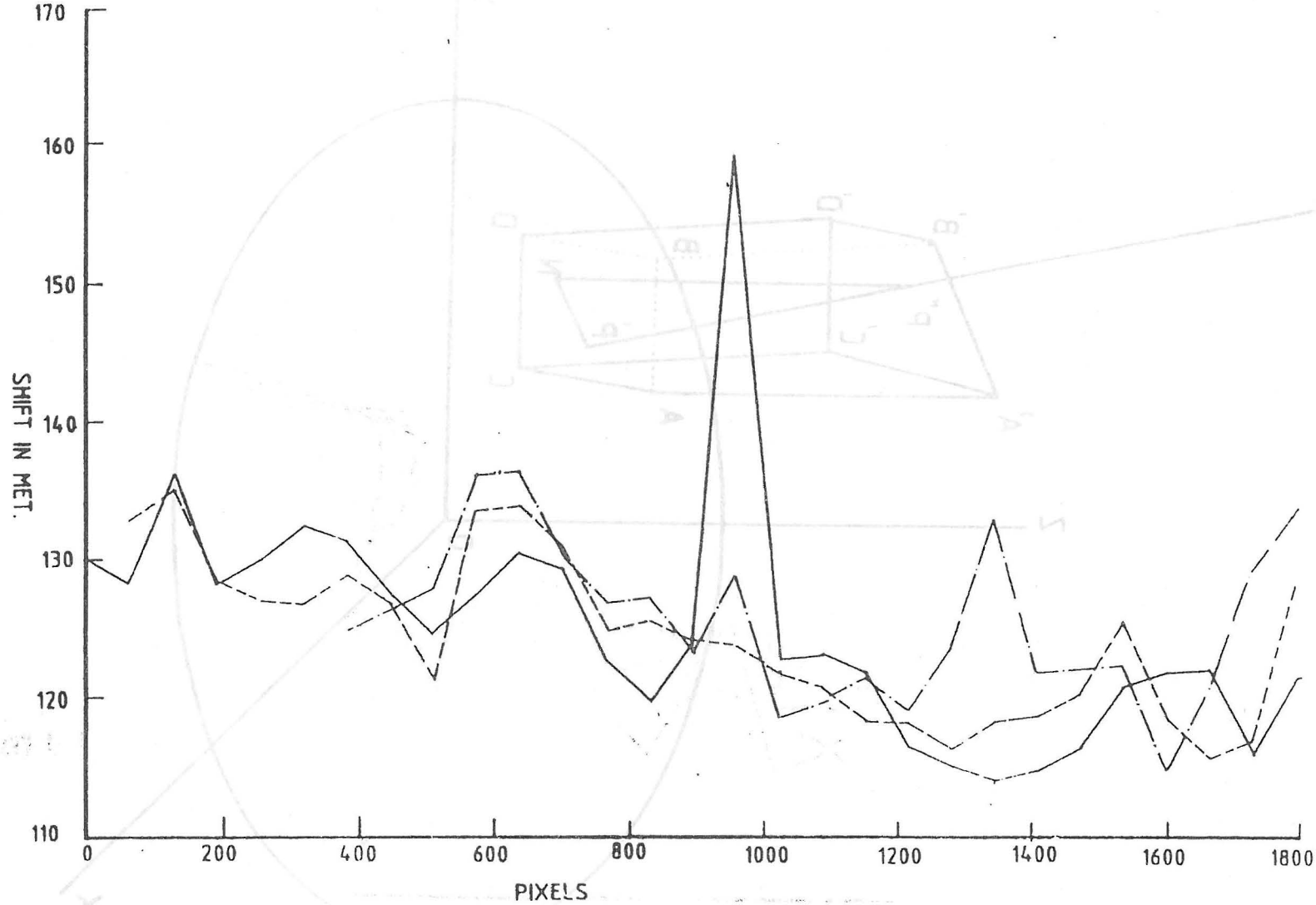
170
160
150
140
130
120
110
SHIFT IN MET.
0
200
400
600
800
1000
1200
1400
1600
1800
PIXELS

FIG. 2

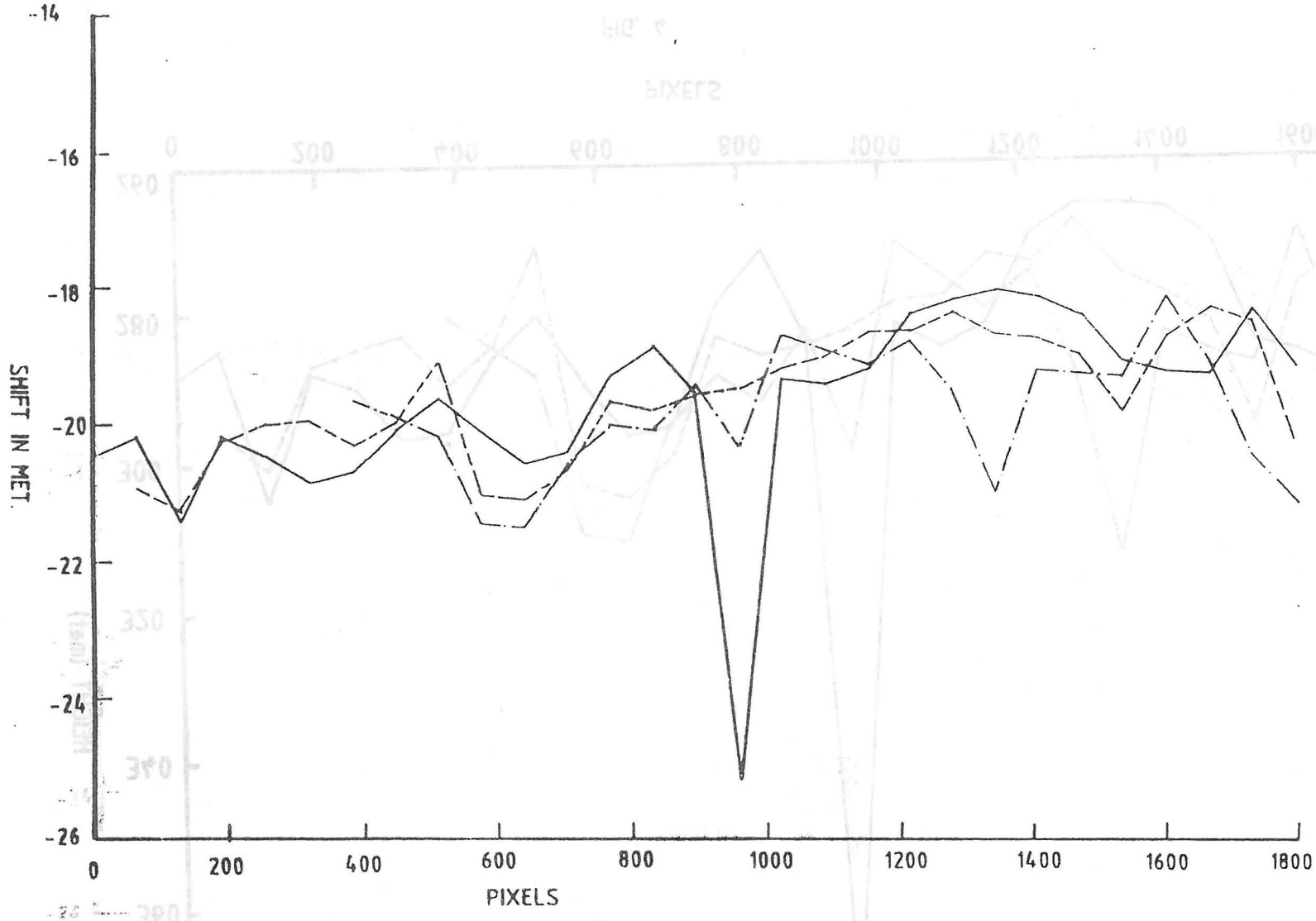
-14
-16
-18
-20
-22
-24
-26
SHIFT IN MET.
0
200
400
600
800
1000
1200
1400
1600
1800
PIXELS

FIG. 3

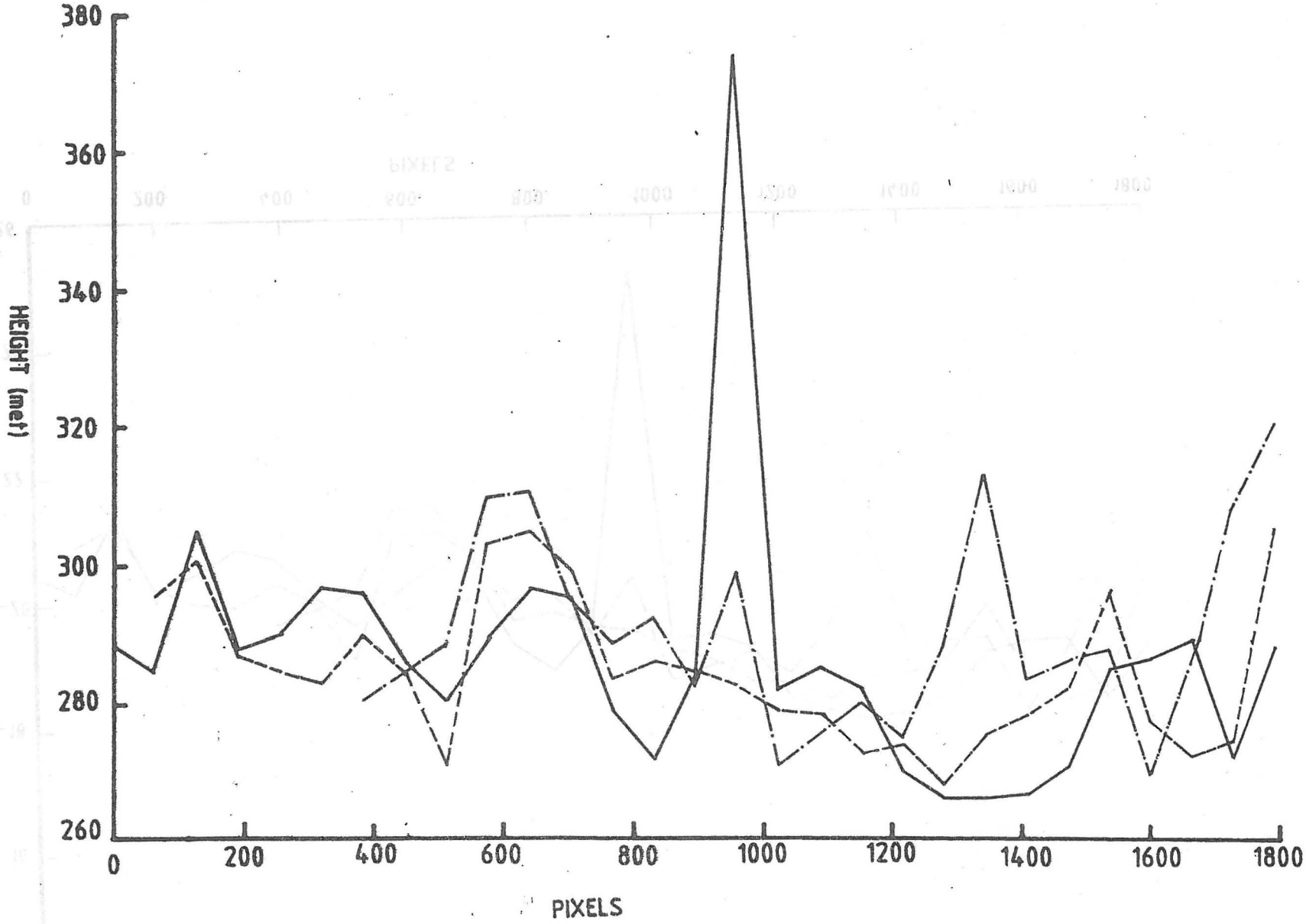
380
360
340
320
300
280
260
HEIGHT (met)
0
200
400
600
800
1000
1200
1400
1600
1800
PIXELS

FIG. 4

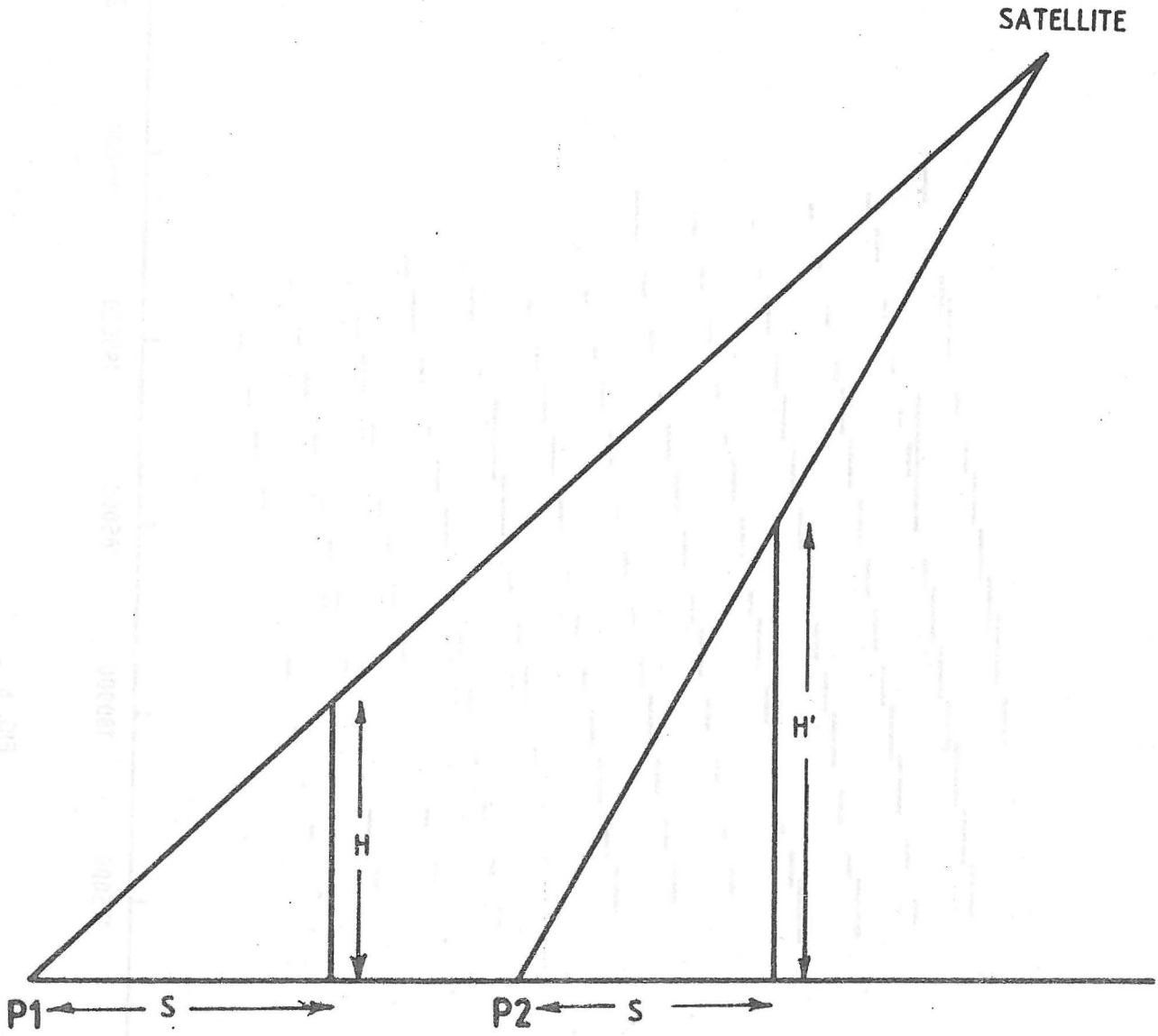

FIG. 5

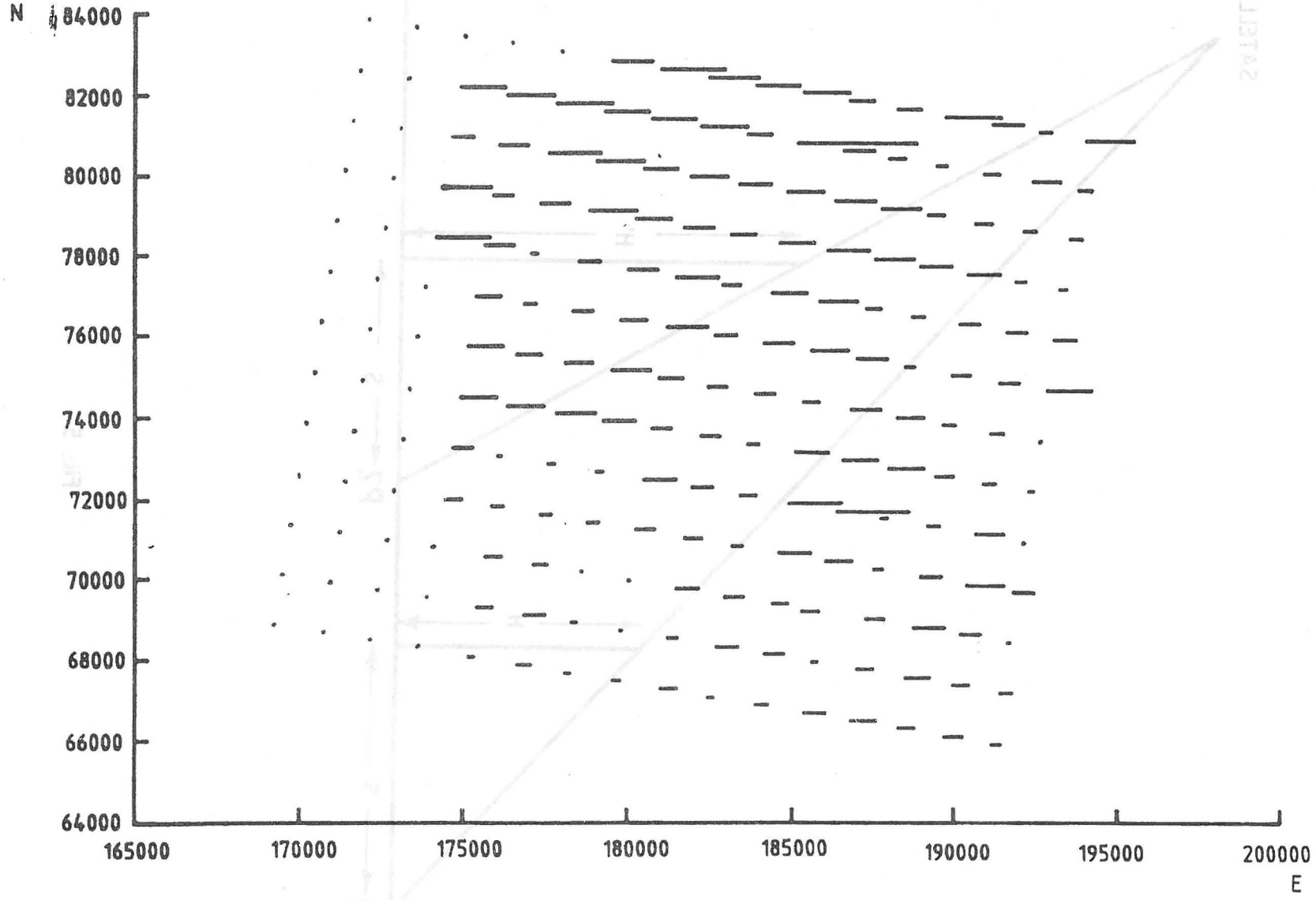
N
84000
82000
80000
78000
76000
74000
72000
70000
68000
66000
64000
165000
170000
175000
180000
185000
190000
195000
200000
E

FIG. 6

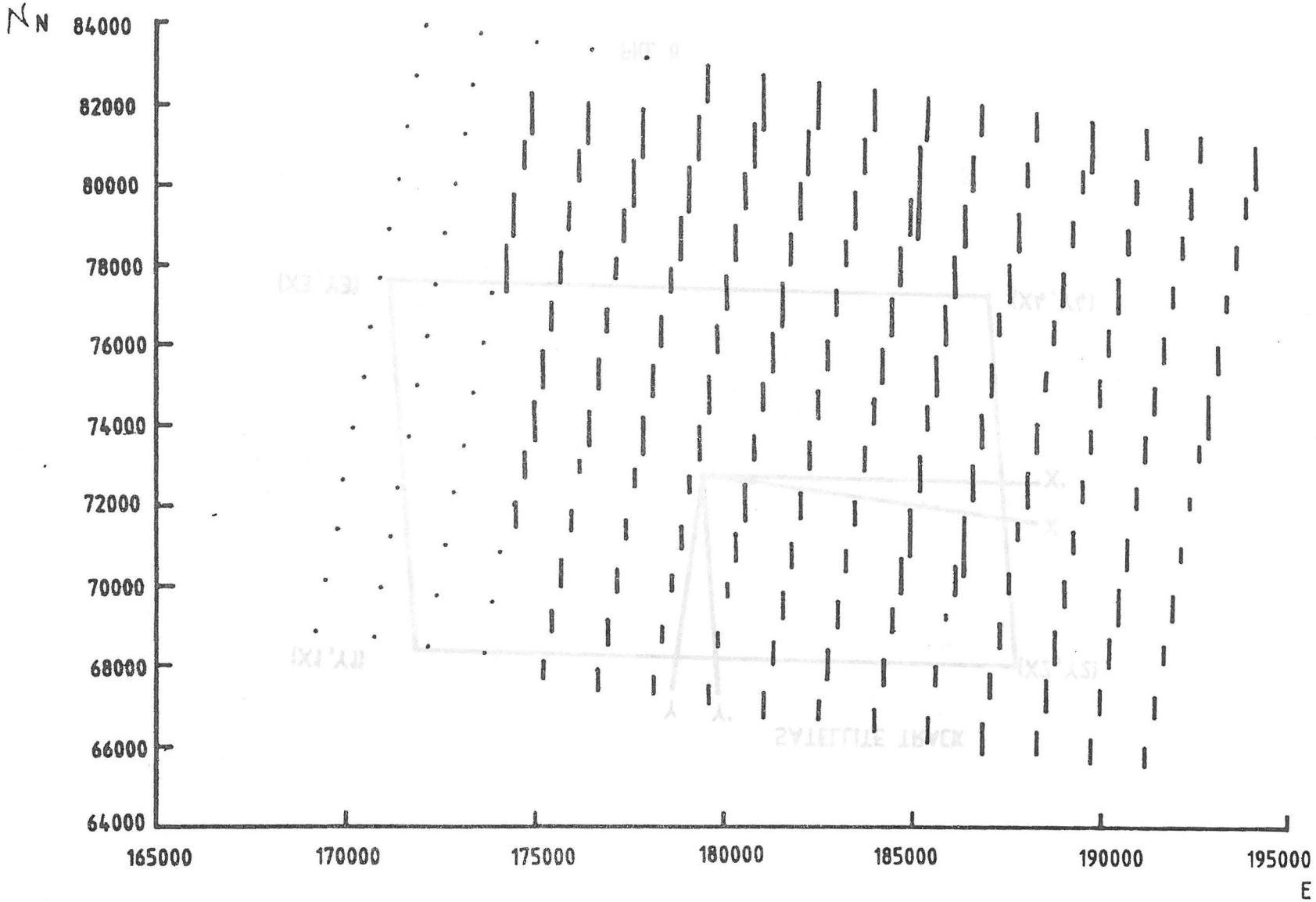
N
N
84000
82000
80000
78000
76000
74000
72000
70000
68000
66000
64000
165000
170000
175000
180000
185000
190000
195000
E

FIG. 7

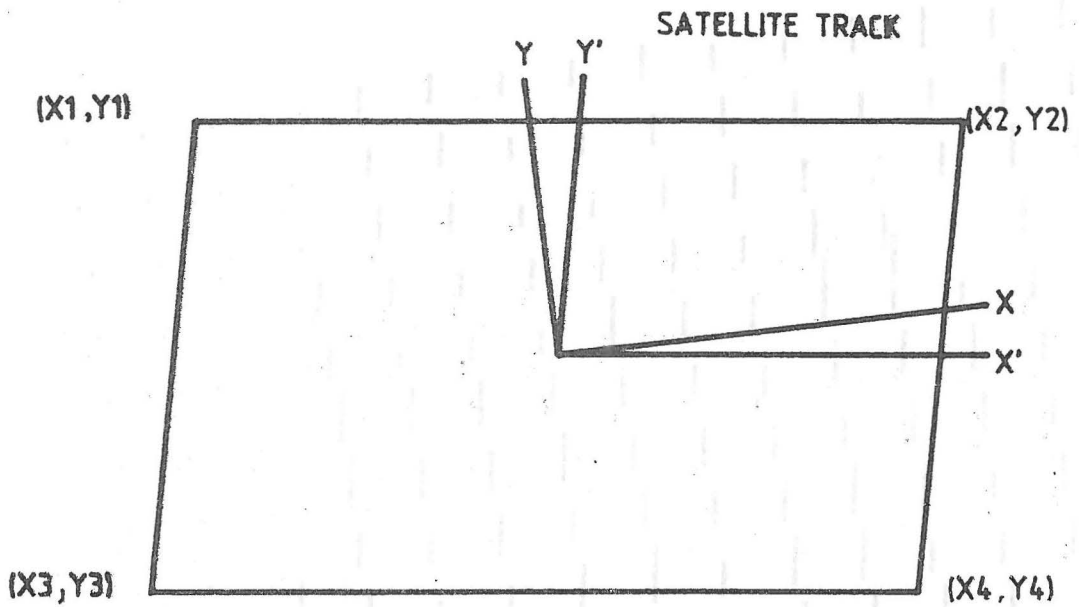

FIG. 8